Particle Simulation for Ion Thruster Grid Design[*†]

[‡]Yasutaka Inanaga and [§]Toshiyuki Ozaki
[‡]Environmental Technology and System Department, Advanced Technology R&D Center
Mitsubishi Electric Corporation
8-1-1, Tsukaguchihonmachi, Amagasaki, Hyogo 661-8861, Japan
+81-6-6497-7586, inanaga@ene.crl.melco.co.jp

[§]Space Engineering Department, Kamakura Works, Mitsubishi Electric Corporation
325, Kamimachiya, Kamakura, Kanagawa 247-8520, Japan

IEPC-01-101

Ion thrusters require a lifetime of over 10,000 hours. The lifetime limitation depends primarily on the erosion of extraction grids. We therefore developed a model that is to predict grid erosion characteristics. This model is based on the Particle In Cell with Monte Carlo Collision (PIC-MCC) method. Sputtering on the screen grid due to doubly-charged ions was taken into account in order to apply the model to the Kaufman-type thruster in a high discharge voltage operation. In addition, the time-dependence grid shape was calculated, and agreed qualitatively with the calculated grid shape and the results of the ETS-6 thruster endurance test.

Nomenclature

I_d = discharge current (mA)
I_b = beam current (mA)
I_{Sc}, I_{Ac}, I_{De} = screen, accel, decel grid current (mA, μA/hole)
j_{Sc}, j_{Ac}, j_{De} = screen, accel, decel grid current density (nA/m^2)
$\dot{m}$ = propellant mass flow rate (sccm)
m_i = ion mass (kg)
n_i, n_e n_n = ion, electron, neutral number density (m^{-3})
n_p = number density of thruster plasma (m^{-3})
n_{ref} = electron number density at reference potential (φ=0)
N_{hole} = total number of grid holes
T_g, T_i, = gas, ion temperature (K)
T_e = electron temperature (eV)
V_d = discharge voltage (V)
Y = sputtering yield (Atoms/Ion)
φ = local potential (V)
φ_{Sc}, φ_{Ac}, φ_{De} = screen, accel, decel grid potential (V)
φ_p = plasma potential (V)
η_u = propellant utilization efficiency without NHC (%)
e = element charge
ε_0 = permittivity of vacuum
r, z, ϕ = cylindrical coordinate

Introduction

Mitsubishi Electric Corporation has developed the 20 mN xenon ion thruster, 13 cm-diameter Kaufman-type (Figure 1) applied for the north south station keeping of GEO satellites. One of the aims in the development of ion thruster is to prolong the lifetime for over 10,000 hours. The most critical factor for this ion thruster lifetime is the erosion of the beam extraction grid, especially the screen grid[1].

Being able to predict ion thruster lifetime is very useful in grid design. Therefore, many numerical simulations describing grid erosion have been presented in the last decade[2,3,4]. In the Kaufman-type ion thruster operating in a high discharge voltage of around 40 V under certain conditions, the erosion of the screen grid caused by

[*]Presented as Paper IEPC-01-101 at the 27th International Electric Propulsion Conference, Pasadena, CA, 15-19 October, 2001.

doubly-charged ions is a lifetime limitation factor. Most of the codes did not consider doubly-ionized state. Even model that considered doubly-charged ions, only focused on accel and decel grid erosion[5].

We modeled the single aperture of the extraction grid system and the adjacent plasma in 2D cylindrical axisymmetry. The code is based on a Particle In Cell with Monte Carlo Collision (PIC-MCC) method for ions and the fluid approach for electrons. The calculation model includes doubly-charged ions in order to consider the erosion of all three grids.

The validity of the model was tested through the quantitative agreement in the screen and accel grid shape change between the calculation and the results of the ETS-6 thruster life test.

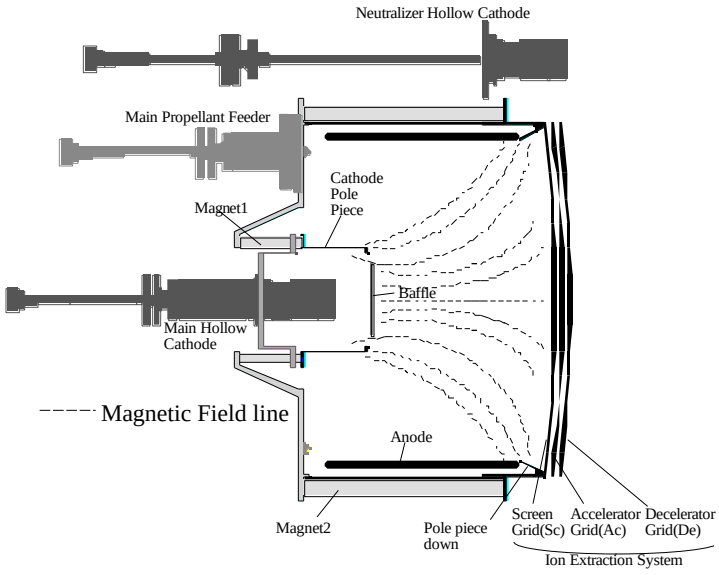

Figure 1. The schematic diagram of the Kaufman-type ion thruster.

Modeling

The modeling is subject to the single aperture set of the extraction grid system and the adjacent plasma, as shown in Figure 2.

Electric Potential

The Poisson equation in 2D cylindrical axisymmetry, as shown below, we solved.

$$\frac{1}{r}\frac{\partial(r\varphi)}{\partial r}+\frac{\partial\varphi}{\partial z}=-\frac{e}{\varepsilon_0}(n_i-n_e)$$

$$\text{upstream: } n_e=n_p\exp\left[\left(\varphi-(\varphi_{sc}+\varphi_p)\right)/T_e\right]$$

$$\text{downstream: } n_e=n_{ref}\exp\left(\varphi/T_e\right)$$

The boundary conditions for the electric potential are shown in Figure 3. The electron density is given by the Boltzmann relationship in the upstream and the downstream region, but different reference potentials and densities are assumed for different regions. The border between the regions is taken to be the upstream face of the accel grid. Neumann conditions are applied to the downstream side of the calculation area and the adjacent aperture set boundary.

The thruster plasma boundary provides the Dirichlet condition, whose value is assumed by the Bohm sheath criterion: $\varphi_{SC}+\varphi_p-T_e/2$, where φ_p is plasma potential, which is assumed to be 5 V higher than the discharge voltage. The Poisson equation has a non-liner term due to exp(φ) of the electron density. We use the multi-dimensional Newton method, and the correction terms are obtained by the SOR scheme.

Ion Motion

Ions move in the 2D space (r,z) and 3D velocity (v_r,v_z,v_ϕ): 2D3v phase space followed by the Particle In Cell (PIC) method. The integration of the motion equation adopts a leapfrog method.

The boundary conditions for ions are shown in Figure 4. New incident ions are injected uniformly due to the Bohm criterion from the upstream border. The radial velocity of the ion is obtained from the Maxwell distribution of the temperature equal to the gas temperature (~500K).

Because the thruster plasma is highly ionized, there are doubly as well as singly-charged ions. The ratio of doubly-charged ion is determined by the function of the discharge voltage, adopted from the experimental results of Takegahara et al.[6].

Neutral Atoms

The neutral atoms treated in the particle code independently. In this code particles collide with the grid surface but do not collide with each other. The boundary conditions for the neutral atoms are shown in Figure 5. The neutral particles are injected uniformly with sonic

velocity in the z-direction at the upstream face of the screen grid. We assumed that the radial velocity is the Maxwell distribution of the gas temperature.

Collision

The ion–neutral collision is modeled by the Monte Carlo Collision (MCC) method. The considered collision mechanisms are charge exchange (CEX), momentum transfer (MT). Each collision cross section is shown in Figure 6. The MT cross section for Xe^{++} with Xe is assumed to the same as Xe^{+}.

Sputtering Yield

The sputtering yield $Y(\varepsilon, \theta)$ is calculated by the function of the energy and collision direction of the ion reached to the grid surface. The yield function is given by the formula of Matsunami et al.[7, 8].

The sputtering yield of the doubly-charged state is assumed to be the same as that of the singly-charged ion.

The procedure for estimating the shape change of the grids is as follows.

0. Divide the grids into small cells that have an initial filling factor of 1.
1. Calculate the neutral density distribution by a given grid shape and the thruster operation parameters.
2. Solve the iterated ion distribution by the PIC-MCC method.
3. Calculate the sputtering rates on the surface of each boundary cell facing the plasma.
4. Determine the "process time", which is at least the filling factor changed from 1 to 0 at each boundary cell.
5. Subtract the normalized erosion depth during the process time from the filling factor of each boundary cell. Then if the filling factors become less than 0, these cells are removed. And negative filling factor adds again to a filling factor of the adjacent cell.
6. Add the process time to the total operation time, continue the calculation by the changed grid shape, and repeat steps 1-6.

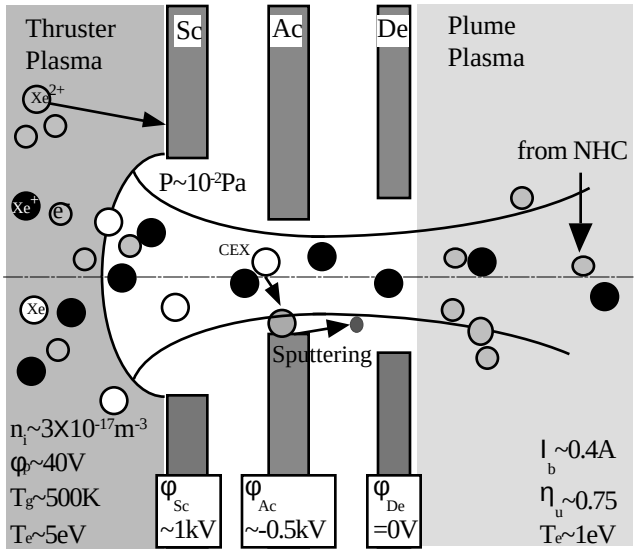

Figure 2. Ion extraction and sputtering model of beam extraction system.

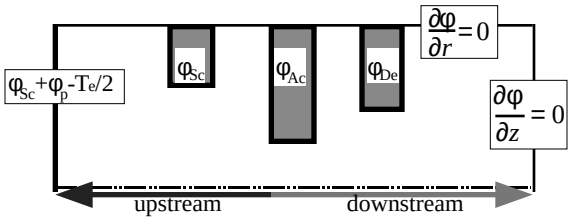

Figure 3. Boundary conditions for electric potential

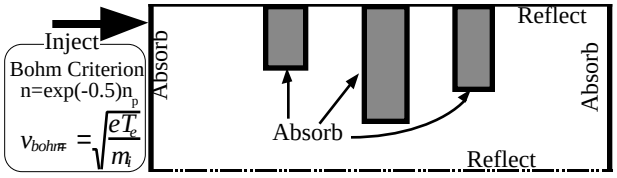

Figure 4. Boundary conditions for ion motion.

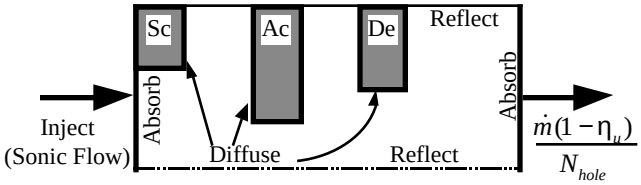

Figure 5. Boundary conditions for neutral particles

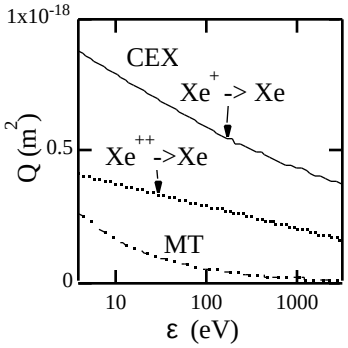

Figure 6. Collision cross section[9,10]

Result

Ion Extraction Characteristics

The neutral density, potential and ion density distribution in the case of the ETS-8 grid set condition[11] are shown in Figures 7, 8 and 9 respectively.

The grid current is shown in Table 1. We determined the thruster plasma density and the electron temperature in order to obtain the same beam current in the experimental value. The accel grid current is of the same order to the experimental result, but only 60% of that value. Thus, it is possible that the code may not completely describe the phenomenon. We also believe that it would also be affected by the misalignment and off-axis of the aperture set in the experimental setup.

Grid Sputtering Characteristics

The current density distribution and the sputtering rate of the screen grid (Sc) in the above ETS-8 case are shown in Figure 10. The discharge voltage is 32.5 V and the Xe^{2+} to Xe^{+} ratio in density is assumed to be 5%. The indicated sputtering rate is to molybdenum surface. The upper graphs indicate the result of the singly-charged ion and the lower set indicates the result for the doubly-charged. The left graphs show the upstream face, the center show the inner side and the right show the downstream face. The current density according to the singly-charged ions on the upstream face indicated about 60 A/m^2, but the sputtering rate was not significant because it did not reach the threshold energy of the sputtering yield. Meanwhile, the result by the doubly-charged ions predicted that the

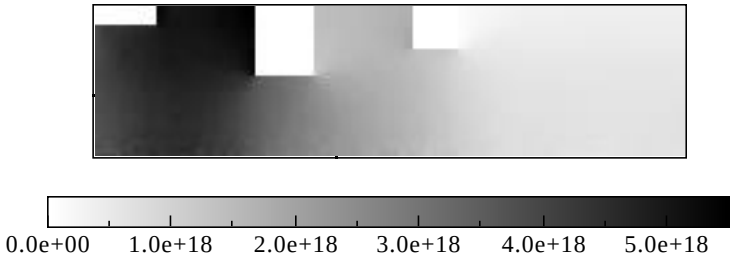

Figure 7. Neutral density distribution (m^{-3})

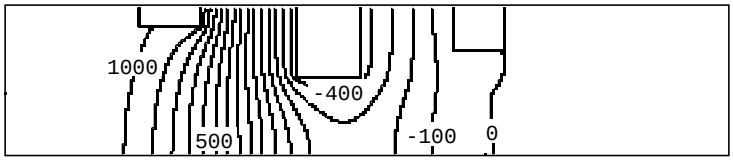

Figure 8. Electric potential distribution (V)

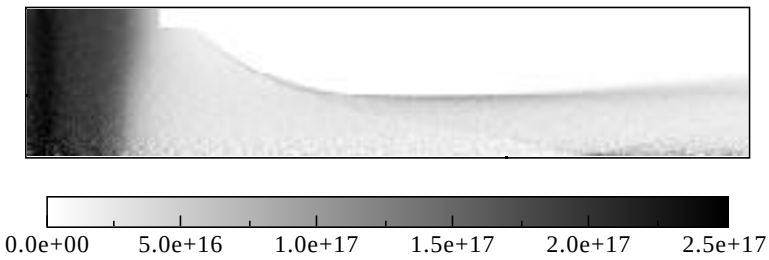

Figure 9. Ion number density (m^{-3})

Table 1. Comparison of Grid current with calculation.

	I_{Sc}	I_{Ac}	I_{De}	I_{beam}
calc.	163mA	1.52mA	0.24mA	468mA
EXP.	–	2.5mA	–	473mA

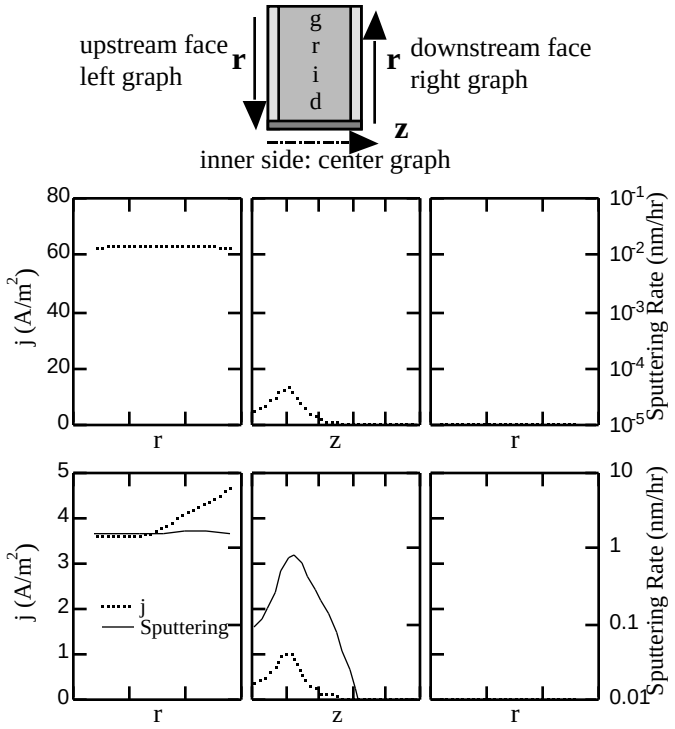

Figure 10. Current density and Sputtering rate on Sc grid (Upper: Singly charged, Lower: doubly-charged)

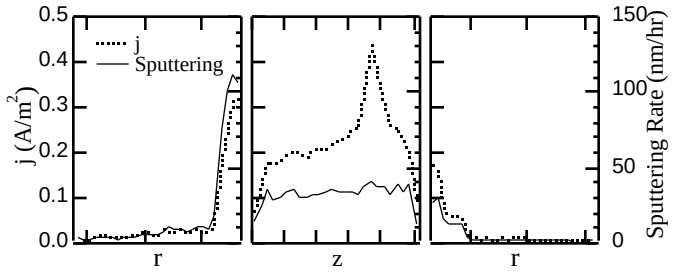

Figure 11. Current density and Sputtering rate on Ac grid

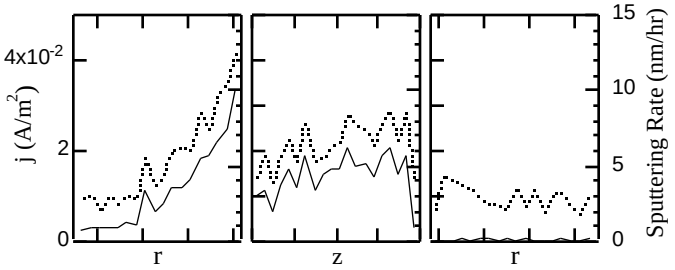

Figure 12. Current density and Sputtering rate on De grid

upstream face is eroded clearly and that the rate is 3.5 μm/10^3hrs. With a discharge voltage of 39.9 V in the other calculation, the estimated sputtering rate exceeded 60 μm/10^3hrs. This value closely agreed with the experimental result of 56 μm/10^3hrs. This reconfirms that the lower discharge voltage increases the long-lifetime characteristics of the screen grid.

The current density distribution and the sputtering rate of the accel grid (Ac) and the decel grid (De) by the singly-charged ion are shown in Figures 11, 12 respectively. The effect by doubly-ionized particle to the sputtering rate is negligible compared to the singly-ionized ion on the accel and decel grid when the retio of Xe^{2+} to Xe^{+} is 5%. This is due to the smaller CEX cross section for the doubly -charged ion compared to that for singly one. In Figure 11 on the upstream face, the significant high current density and the sputtering rate appear on the center side rim on the inner side. In this region the sputtering rate reaches approximately 120 nm/hr. The current density is higher than the other surfaces and the distribution profile has a peak located at one third of the thickness from the downstream grid face, but the sputtering rate profile is broad, as the ions contributed to the current peak have a low energy.

Eroded Shape in Endurance Test

Figure 13 shows the calculated grid shape change under the operation condition of the ETS-6 endurance test. The discharge voltage was quite high (around 40 V). In an actual condition, the screen and the accel grid are coated by the anti-sputtering ceramic, however we cannot yet adopt the coating in the calculation. The sectional ETS-6 grid shape after 7000 hours of operation in the endurance test[12] is shown in Figure 14. The calculated sectional shape is similar to the experimental result except for the center side edge of the upstream and downstream accel grid. This calculation failed in a 6879 hours thruster operation, when the screen grid completely eroded. We think the anti-sputtering coating causes the difference in the shape and the shorter forecast failure time.

In addition, we have not treated the re-deposited particles on a grid by the sputtered particles. As shown in Figure 14, depositing is significant on the decel grid upstream face, but it is not presented in the calculation. Our future work will be to estimate the re-deposition, which is related to the production of the flakes, which cause short-circuits

between the grids.

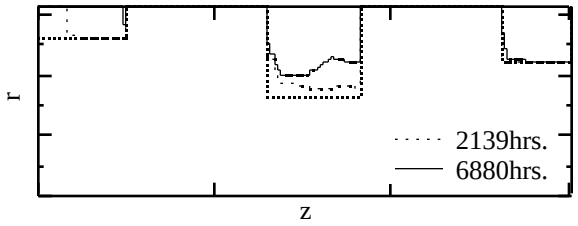

Figure 13. Calculated grid shape change in the ETS-6

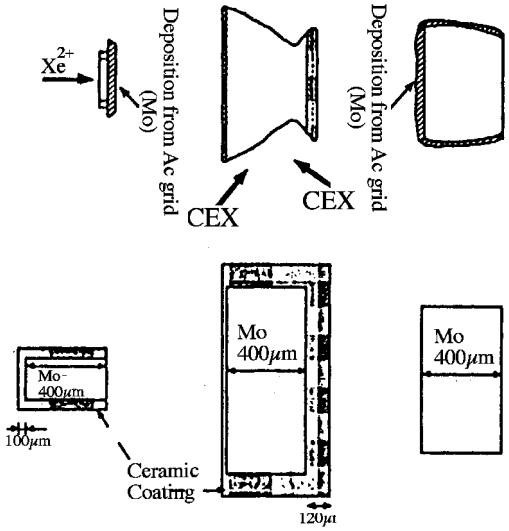

Figure 14. Sectional shape of the ETS-6 grid after the endurance test
(initial: below, after 7,000 hours operation: above).

Conclusions

A particle simulation code was developed to investigate the grid erosion of the ion thruster. The procedure includes the time-dependence of the grid shape change and the effect of doubly-charged ion sputtering. The calculated grid current had the same level as the experimental value, and the calculations and the result of the ETS-6 thruster endurance test in the grid erosion shape agreed qualitatively.

It was confirmed that the dominant factor is the doubly-charged ion sputtering in the screen grid erosion, when discharge voltage is around 40 V. The sputtering caused by Xe^{++} can be neglected compared with the erosion by Xe^{+} in the accel and decel grid.

However, many aspects of the model must be improved. An important problem is the anti-sputtering ceramic coating on the grid shaped like the ETS-6 thruster, which results in a different shape and a shorter forecast time. Another point to be addressed is to determine where the eroded particles, and how many, are blasted and re-deposited on the grid.

References

[1] T. Ozaki et al., "Improvement of 20mN Xenon Ion Thruster," IEPC-99-153.

[2] R. A. Bond and P. M. Latham, "Ion Thruster Extraction Grid Design and Erosion Modeling using Computer Simulation," AIAA-95-2923.

[3] T. Shiraishi et al., "Numerical Simulation of Grid Erosion for Ion Thruster," IEPC-95-90.

[4] X. Peng, W. M. Ruyten and K. Dennis,"Charge Exchange Grid Erosion Study for Ground-based and Space-based Operations of Ion Thruster," IEPC-93-73.

[5] I. D. Boyd, M. W. Crofton, "Computational Study of Grid Erosion Through Ion Impact," AIAA-00-3664.

[6] H. Takegahara et al., "Beam Characteristics Evaluation of ETS-VI Xenon Ion Thruster," IEPC-93-235.

[7] N. Matsunami et al., "Energy Dependence of the Ion-induced Sputtering Yields of Monatomic Solids," Atomic Data and Nuclear Data Tables 31, 1-80 (1984).

[8] Y. Yamamura et al., "Angular Dependence of Sputtering Yields of Monatomic Solids," IPPJ-AM-26, Institute of Plasma Physics, Nagoya University (1983).

[9] D. E. Hastings and D. Oh, "Computational Modeling of Expanding Plasma Plume in Space Using PIC–DSMC Algorithm," Final Technical Report for F49620-95-1-0319 (1997).

[10] S. Pullins et al., "Ion Dynamics in Hall Effect and Ion Thruster: Xe^{+}+Xe Symmetric Charge Transfer," AIAA-00-0603

[11] T. Ozaki et al., "Development Status of Xenon Ion Thruster for ETS-8," ISTS-2000-b-12.

[12] S. Simada et al., "Ion Thruster Endurance Test Using Development Model Thruster for ETS-VI," IEPC-93-169.